Stepwise transition from the Eocene greenhouse to the Oligocene icehouse

MIRIAM E. KATZ[1,2]*, KENNETH G. MILLER[2], JAMES D. WRIGHT[2], BRIDGET S. WADE[3,4], JAMES V. BROWNING[2], BENJAMIN S. CRAMER[5] AND YAIR ROSENTHAL[2,3]

[1]Department of Earth and Environmental Science, Rensselaer Polytechnic Inst., Troy, New York 12180, USA
[2]Department of Earth and Planetary Sciences, Rutgers University, Piscataway, New Jersey 08854, USA
[3]Institute of Marine and Coastal Science, Rutgers University, 71 Dudley Road, New Brunswick, New Jersey 08901, USA
[4]Department of Geology and Geophysics, Texas A&M University, College Station, Texas 77840, USA
[5]Department of Geological Sciences, 1272 University of Oregon, Eugene, Oregon 97403-1272, USA
*e-mail: katzm@rpi.edu

Published online: 13 April 2008; doi:10.1038/ngeo179

In the largest global cooling event of the Cenozoic Era, between 33.8 and 33.5 Myr ago, warm, high-CO_2 conditions gave way to the variable 'icehouse' climates that prevail today. Despite intense study, the history of cooling versus ice-sheet growth and sea-level fall reconstructed from oxygen isotope values in marine sediments at the transition has not been resolved. Here, we analyse oxygen isotopes and Mg/Ca ratios of benthic foraminifera, and integrate the results with the stratigraphic record of sea-level change across the Eocene–Oligocene transition from a continental-shelf site at Saint Stephens Quarry, Alabama. Comparisons with deep-sea (Sites 522 (South Atlantic) and 1218 (Pacific)) $\delta^{18}O$ and Mg/Ca records enable us to reconstruct temperature, ice-volume and sea-level changes across the climate transition. Our records show that the transition occurred in at least three distinct steps, with an increasing influence of ice volume on the oxygen isotope record as the transition progressed. By the early Oligocene, ice sheets were ~25% larger than present. This growth was associated with a relative sea-level decrease of approximately 105 m, which equates to a 67 m eustatic fall.

The greenhouse-to-icehouse transition across the Eocene–Oligocene (E–O) boundary (33.7 Myr) was a critical shift in Cenozoic climate marked by declining atmospheric CO_2 (ref. 1), long-term deep-sea cooling[2,3], thermal isolation of Antarctica[4] and establishment of large ($>25 \times 10^6$ km^3) Antarctic ice sheets[5–9]. Smaller, transient glaciations occurred in the middle and late Eocene[10–13]; eventually, the balance tipped from the greenhouse mode to the icehouse mode in the earliest Oligocene. Accelerated biotic turnovers in marine and terrestrial flora and fauna were associated with this transition[14,15]. Documenting the roles of ice-sheet and temperature fluctuations is vital to understanding the past global climate system and the system response to changes during significantly warmer climates. Yet, despite decades of research, there still is substantial uncertainty about the magnitude of global ice-volume versus temperature change during the E–O transition because of (1) uncertainties in, and limitations of, palaeoceanographic proxies and (2) insufficient number of proxies at a single location to fully constrain system changes.

The E–O transition is marked by a major positive excursion (1.0–1.5‰) in the oxygen isotopic values recorded in the tests of benthic foraminifera ($\delta^{18}O_{bf}$), first documented decades ago[16]. Subsequent studies proposed that this transition was more complex, occurring in two steps: a 0.5‰ increase (the 'precursor event', ~33.8 Myr), followed by the Oi-1 ('Oligocene isotope event 1') 1.0‰ increase[8,17,18]. The age of Oi-1 (33.545 Myr) has been constrained palaeomagnetically to the Chron C13r/C13n transition at Site 522 (refs 19–21), Site 744 (ref. 7) (Indian Ocean) and Saint Stephens Quarry (SSQ) (refs 18,22). Previous studies used too few proxies to constrain the amount of cooling, ice-volume increase and sea-level fall[8,17,18]. Here, we report all three components ($\delta^{18}O$, Mg/Ca, sequence stratigraphy–sea level) from a single continental shelf location, SSQ, with well-preserved foraminifera and excellent age control (see Methods section; Supplementary Information, Notes and Table S1). Using these proxies, we constrain all three components to capture a detailed record of the sequence of events that constitute the greenhouse-to-icehouse climate transition that occurred from ~34–33.5 Myr, including a previously unidentified event between the precursor and Oi-1 shifts. Comparison with the only detailed deep-sea records of Mg/Ca and $\delta^{18}O_{bf}$ (Sites 522 and 1218) across this interval is critical to constraining the $\delta^{18}O$ of seawater (δ_w) during these stepwise events.

INTEGRATED PROXIES

Multiple proxies are needed to constrain temperature, ice-volume and sea-level changes because multiple environmental parameters can affect each proxy. The first proxy is $\delta^{18}O_{bf}$, which is a function of both the temperature and the δ_w in which the foraminifera calcified. In turn, δ_w is a function of (1) global ice volume and (2), for shelf and surface waters, local–regional river-water input and evaporation–precipitation patterns. The second proxy is Mg/Ca measurements of foraminiferal shells, which provide the potential to independently reconstruct water temperature (thereby constraining one influence on $\delta^{18}O_{bf}$), because the uptake of Mg into foraminiferal $CaCO_3$ is temperature dependent. The third proxy is the stratigraphic record of sea-level change (a function of ice-volume change over thousands to a few million years) that is reconstructed from local–regional palaeodepth variations

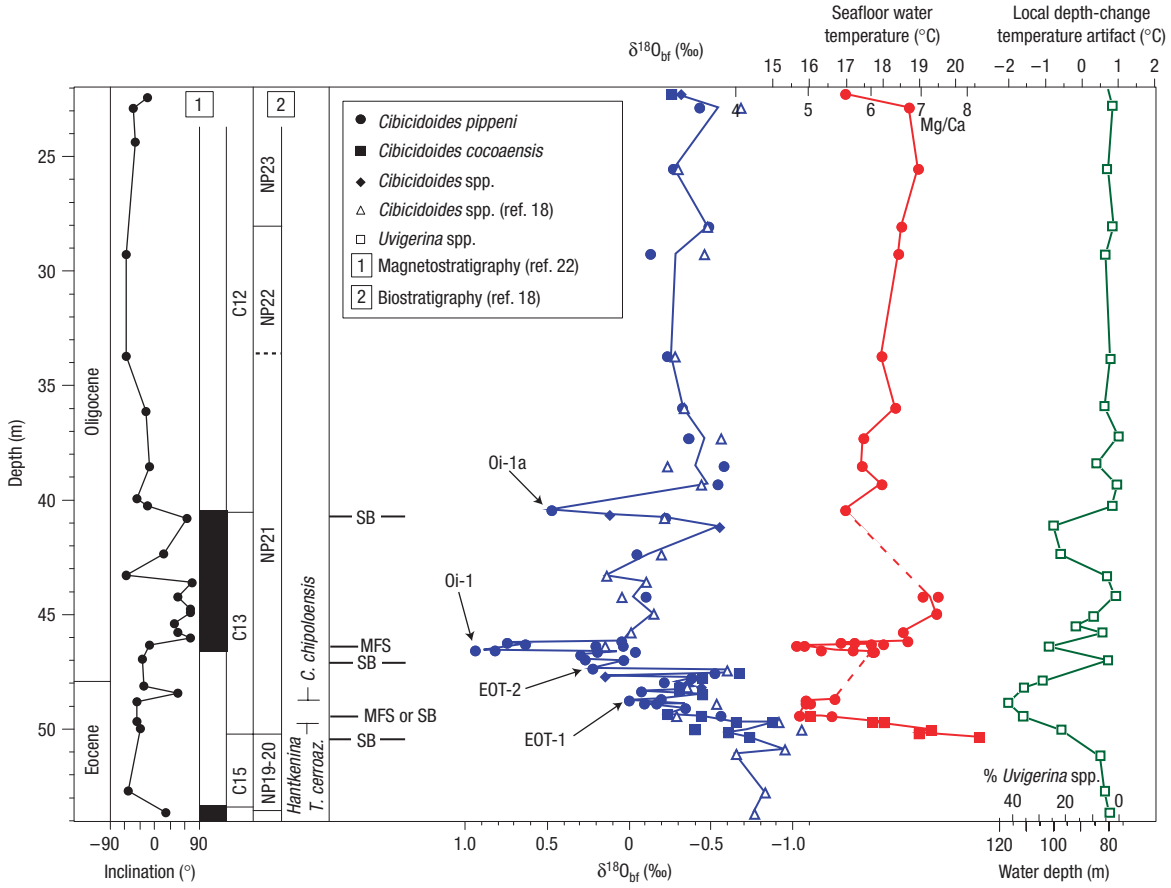

Figure 1 SSQ proxy data for ice volume, temperature and sea level. $\delta^{18}O$ and Mg/Ca were measured on benthic foraminifera (see Supplementary Information, Table S2). Multiple analyses of single samples are shown, connected with a line through average values. *Uvigerina* abundances were used to estimate palaeodepth and the local temperature change driven by water-depth changes (see the text). MFS = maximum flooding surface (deepest palaeodepth within a sequence). SB = sequence boundary (forms during sea-level fall), at ~50.3 m (33.9–35.0 Myr), 47 m (33.59–33.62 Myr) and 40.5 m (33.0 Myr).

(determined from biofacies and lithofacies in shallow-water settings), correcting for effects of sediment compaction, loading and subsidence[6].

Conflicting reconstructions of the greenhouse-to-icehouse transition have resulted from limitations of geochemical proxies. Benthic foraminiferal Mg/Ca-derived temperature reconstructions from deep-sea sites indicate that no cooling occurred across the Oi-1 event, leading to the hypothesis that the $\delta^{18}O_{bf}$ increase was caused solely by ice-volume expansion[23]. However, the Mg/Ca record from deep-sea sediments[17,24] may be biased by a sharp increase in carbonate saturation in the world's oceans at this time, marked by the deepening of the calcite compensation depth[8,25]. At odds with the Mg/Ca–temperature estimates, continental records indicate that tropospheric temperatures decreased by ~8 °C (refs 26,27). Ice-volume change has been independently estimated from integrated $\delta^{18}O_{bf}$ and sequence stratigraphy (on the assumption that sea-level fall results from water transferred from oceans to continental ice sheets during ice-sheet growth). These studies found that during the Oi-1 $\delta^{18}O_{bf}$ increase, global sea level fell by ~55 ± 15 m, with no detectable fall associated with the precursor event[6,18,28]. Without a direct temperature proxy, Miller and colleagues[18] built on these findings to propose a 2 °C cooling during the precursor, and 2–4 °C cooling during Oi-1.

Hence, substantial uncertainty remains over the amount of temperature, ice-volume and sea-level change that occurred across the critical shift to the icehouse climate. Integrating $\delta^{18}O_{bf}$, Mg/Ca and sequence stratigraphic records from a single unaltered section that was well above the calcite compensation depth provides the potential to resolve the succession of events that led to continental-scale Antarctic ice-sheets. Here, we measure $\delta^{18}O_{bf}$ and Mg/Ca at SSQ and directly tie these geochemical data to independent records of sea-level change at the same location (Fig. 1; Methods section). We capitalize on the continuously cored section at the continental-shelf SSQ location with a higher sedimentation rate (~14.4 m Myr^{-1}) than at deep-sea sites 1218 (8.6 m Myr^{-1}) or 522 (6.7 m Myr^{-1}) across the E–O boundary section. This study builds on the established SSQ framework of lithostratigraphy, sequence stratigraphy, biofacies analysis, magnetobiostratigraphy and low-resolution isotopic stratigraphy that correlated two $\delta^{18}O_{bf}$ increases to the global Oi-1 and precursor events[18]. Our higher-resolution data reveal additional structure to the events that constitute this transition, including a previously unidentified step to an intermediate climate state.

In this region of the Gulf of Mexico, both modern and late Eocene–early Oligocene hydrography suggests a temperature gradient of ~1 °C/15 m (refs 29–31). Therefore, in addition to global/regional temperature variations through time, bathymetric adjustments to sea-level changes should have caused small changes in temperature that may have influenced SSQ $\delta^{18}O_{bf}$. To account for this, we used abundances of the benthic foraminifera *Uvigerina*

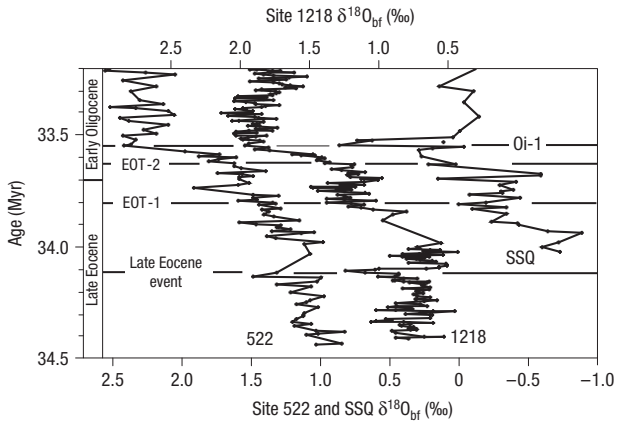

Figure 2 Comparisons of $\delta^{18}O_{bf}$ from Site 522 (ref. 7), Site 1218 (ref. 8) and SSQ (see Supplementary Information, Table S2). Duplicate analyses are averaged. See Supplementary Information for age model parameters. We define a series of $\delta^{18}O_{bf}$ events (EOT-1 and EOT-2; see the text for details) that comprise the Eocene–Oligocene climate transition that culminated in the Oi-1 event.

to estimate palaeodepth[18] (Fig. 1); palaeodepth was then used to estimate the temperature change driven by local water-depth changes, on the basis of modern and late Eocene–early Oligocene temperature profiles[29–31]. The SSQ record does not seem to have been affected by local changes in δ_w, on the basis of several observations. First, in the modern Gulf of Mexico off Alabama, variations in δ_w are limited to between 50 and ~100 m because salinity variations are very small (36.4 to 36.5‰), with a stable δ_w/salinity slope of ~0.1/psu (ref. 32). Second, Eocene regional gradient reconstructions were similarly low[31], indicating that the δ_w contribution to the $\delta^{18}O_{bf}$ record was largely a global δ_w signal. We note that the SSQ $\delta^{18}O_{bf}$ patterns are remarkably similar to deep-sea Eocene–Oligocene boundary sections[8,17], with lower $\delta^{18}O_{bf}$ values that reflect the warmer shelf temperatures[18]. This indicates that SSQ recorded the global $\delta^{18}O_{bf}$ signal without being masked by local effects, and supports the validity of using shallow-water sections to monitor the magnitude of global events, even if there may be a distinguishable local signal also recorded in the data.

STEPS OF THE GREENHOUSE-TO-ICEHOUSE TRANSITION

A late Eocene event (~34.1 Myr) that preceded the E–O climate transition is marked at Sites 522 and 1218 by a transient ~0.5‰ $\delta^{18}O_{bf}$ increase that returned to pre-excursion values (we follow ref. 5 in defining events on $\delta^{18}O$ maxima) (Fig. 2, Table 1). This event is not recorded at SSQ because of a hiatus due to sea-level fall. The only Mg/Ca record across this event (Site 1218 (ref. 17)) shows no significant change, suggesting that this was primarily an ice-volume event, consistent with the hiatus at SSQ and sea-level fall of ~40 m (see sea-level-to-δ_w calibration below). This supports our contention that events recorded at the deep-sea sites are also evident in SSQ records.

Following this ice-volume increase, evidence for substantial glacial ice melting is recorded in a δ_w decrease at SSQ (~0.7‰) and Sites 1218 and 522 (~0.5‰) (Fig. 3). Consistent with this, there is a shift to deeper-water *Uvigerina*-dominated biofacies at SSQ (Fig. 1). These cooler waters were recorded in Mg/Ca as a 2.5 °C local cooling at SSQ before subsequent global cooling, consistent with the local temperature effect predicted from

Table 1 Summary of changes associated with the Eocene–Oligocene climate transition. Numbers are reported from SSQ, except where indicated (there is a hiatus across the late Eocene event at SSQ).

Event	$\delta^{18}O_{bf}$ increase (‰)	Cooling (°C)	SL fall (m)
Oi-1 (33.545 Myr)	1.0	2	105
EOT-2 (33.63 Myr)	0.8	No data	>0
EOT-1 (33.8 Myr)	0.9	2.5	30
Late Eocene (34.1 Myr)	0.5*	0†	40

*Sites 522 and 1218.

†Site 1218.

water-depth increase (~49.8–50.3 m, Fig. 1). SSQ $\delta^{18}O_{bf}$ data show no significant change associated with this local cooling, most likely because the local $\delta^{18}O_{bf}$ increase (due to cooler, deeper waters) and the global δ_w decrease (due to ice melting) essentially cancelled each other out.

This melting was followed by the first step of the climate transition, observed at all three locations and called the 'precursor' $\delta^{18}O_{bf}$ event (33.8 Myr). We rename this event 'EOT-1' for 'Eocene–Oligocene Transition event 1'. EOT-1 is marked at SSQ by a 0.9‰ $\delta^{18}O_{bf}$ increase and 2.5 °C cooling (Fig. 1, ~49–49.8 m). Site 522 shows a similar cooling (2.0 °C), and all three locations record a δ_w increase of ~0.4‰. This δ_w increase is associated with a small sea-level fall (~30 m; see calibration below). Published sequence stratigraphic analyses at SSQ did not reveal a sea-level fall at this time; however, this minor sea-level change would not be dramatic in the ~75–100 m palaeodepth of this section. A glauconite bed (~49 m) at SSQ associated with EOT-1 may represent a previously undetected hiatus. A global sea-level fall at this time is supported by a coeval erosional event in the Priabonian type section[33] in facies more sensitive to small sea-level changes. These records provide the first direct evidence of both global cooling and minor sea-level fall during EOT-1.

Following EOT-1, a partial return towards pre-event conditions at SSQ with a 0.7‰ $\delta^{18}O_{bf}$ decrease and 0.4‰ δ_w increase occurs in a shallowing-upward succession (Fig. 1; ~47.6–49 m). This pattern is consistent with (but of slightly higher magnitude than) the 0.5‰ $\delta^{18}O_{bf}$ (refs 8,17) and 0.3‰ δ_w decrease at Site 1218 following EOT-1 (Figs 2, 3). This partial return highlights the instability in climate systems during this transition between climate states.

The second step of the transition is 'EOT-2' (~33.63 Myr). This previously unidentified event is marked at SSQ by a clear and sustained ~0.8‰ $\delta^{18}O_{bf}$ increase in the earliest Oligocene (Fig. 1, ~47.4 m), and we note that it is also apparent at Sites 522 and 1218 (~0.4‰) (Fig. 2). Rare benthic foraminiferal occurrences made it unfeasible to analyse for Mg/Ca in this interval (in contrast, smaller sample volume is sufficient for $\delta^{18}O_{bf}$); therefore, it is impossible to apportion the 0.8‰ between ice volume and temperature with certainty on the basis of geochemical records alone. Nonetheless, it occurs within a shallowing-upward environment to the sequence boundary at SSQ (with no detectible hiatus), indicating that falling sea level (and hence ice-volume increase) most likely was a component of the EOT-2 shift. In strong support of our speculation, δ_w values began to increase at Sites 522 and 1218 at this time (Fig. 3).

The earliest Oligocene Oi-1 event (33.545 Myr) is the culmination of the greenhouse-to-icehouse transition. It is marked by a ~1‰ $\delta^{18}O_{bf}$ increase at SSQ and Sites 522 and 1218, and by the beginning of a ~2 °C cooling indicated by Mg/Ca data at SSQ (Figs 1, 2). This indicates that up to half of the $\delta^{18}O_{bf}$ increase at Oi-1 was due to ice-volume increase, and the other half to cooling.

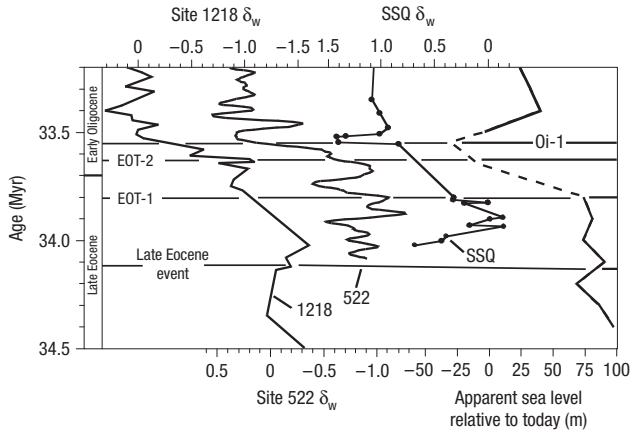

Figure 3 Comparisons of δ_w from Site 522, Site 1218, and SSQ with sea level. All δ_w were calculated for this study (see the Methods section). Once corrected, we estimate that the δ_w across the Eocene–Oligocene climate transition was $\sim 1.2 \pm 0.3$‰ at deep-sea and shelf locations (see the text for details). The apparent sea-level record shown here is derived by assuming that a 55–70 m eustatic change[6] corresponds to a change in the volume of the oceans equivalent to 82–105 m (correcting for isostatic loading and assuming full compensation; see the text for details).

The next major ice-volume event of the Oligocene was Oi-1a (~33 Myr) (ref. 5). Our data firmly establish that there was a ~1.0‰ $\delta^{18}O_{bf}$ increase (Fig. 1) associated with the C13n/C12r transition at SSQ (33.058 Myr) (ref. 18), correlating this event with the global Oi-1a fall. In spite of sparse Mg/Ca data in this interval (due to sparse benthic foraminifera), our data show for the first time that the ~40–50 m eustatic lowering that occurred during Oi-1a (refs 6,28) was associated with an overall cooling of ~2 °C (~41–44 m). Therefore, as with Oi-1, about half of the $\delta^{18}O_{bf}$ increase at Oi-1a was due to ice-volume increase, and the other half to cooling.

This succession of events shows that the greenhouse-to-icehouse transition was a complex series of ice-volume, sea-level and temperature events, with increasing influence of ice-volume and sea-level change. EOT-1 (33.8 Myr) was dominated by significant cooling, with a small sea-level fall, and a partial return towards pre-event conditions. The subsequent, newly identified EOT-2 resulted from a combination of sea-level and ice-volume changes, possibly with a temperature component, shifting to a new climate state. In the final step of the transition, the major Antarctic ice sheet expanded to continental-scale at Oi-1, with a 2 °C cooling.

ESTIMATES OF ICE-VOLUME AND SEA-LEVEL CHANGE

We estimate that the global change in δ_w across the Eocene–Oligocene climate transition was ~1.2‰, on the basis of all three locations (Fig. 3). Despite sparse Mg/Ca data in the EOT-2 interval at SSQ, there is a well constrained δ_w increase of $\sim 1.2 \pm 0.3$‰ between the average isotopic minimum at ~33.9 Myr and the Oi-1 isotopic maximum at 33.55 Myr. Site 1218 has a higher-amplitude δ_w change (~1.65‰) across the same interval, but the Mg/Ca record was biased by the change in deep-sea carbonate saturation with the deepening of the calcite compensation depth (ref. 17). The magnitude of this effect was estimated to be ~2 °C (0.44‰) (ref. 17), suggesting a corrected δ_w increase at Site 1218 of ~1.2‰. Site 522 shows a ~1.5‰ change in δ_w (calculated for this study; see Methods section). The magnitude of the carbonate ion bias at the intermediate-depth Site 522 has been estimated to be less than at the deeper Site 1218 (ref. 17). Our calculations show the effect to be ~0.3‰.

Constraining the change in δ_w has implications for interpretations of the ice-volume and temperature history of the greenhouse-to-icehouse transition. (1) The greenhouse-to-icehouse climate transition occurred in a series of steps, with increasing influence of ice-volume and sea-level change. We speculate that these steps are related to a higher-order cyclicity that is hinted at in the data, but cannot be quantified in the short SSQ record using spectral analysis. (2) A 1.2‰ δ_w increase indicates a sea-level fall of ~120–135 m (using the Pleistocene sea-level/$\delta^{18}O$ calibration of 0.11‰/10 m (ref. 34), or the Oligocene 0.1‰/10 m (ref. 35)). The stratigraphic record does not support such a large event (ref. 6).

We reconcile the apparent contradiction in (2) by comparing the δ_w and sea-level records (Fig. 3). Directly calibrating the eustatic estimate of 55 m to the 1.2‰ δ_w increase would require a calibration of 0.22‰/10 m and mean ice-sheet $\delta^{18}O$ lower than −86‰, which is not reasonable (for comparison, modern ice-sheet $\delta^{18}O$ is ~−35 to −60‰ (ref. 36)). Similar calculations for the upper limit of the eustatic estimate (70 m) would require a calibration of 0.17‰/10 m and ice sheets with an average of −68‰, which is not realistic either. However, previous estimates of a 55–70 m eustatic change take into account the isostatic response of the oceanic lithosphere to the change in weight of the overlying water (hydroisostasy), which means that the actual water-volume change from transferring ocean water to glacial ice is ~33% higher than the eustatic change, and this difference accounts for part of the δ_w change. Hence, the 55–70 m eustatic change corresponds to a change in the volume of ocean water of ~82–105 m (correcting for isostatic loading and assuming full compensation (ref. 35)). Using this range, we calibrate δ_w to water volume (rather than to eustasy), yielding 0.12‰/10 m and ice storage that is the equivalent of 105 m water-volume change and a mean ice-sheet $\delta^{18}O$ of −45‰.

Our δ_w estimates and recalibration correspond to ice sheets that were ~25% larger than they are today. This is reasonable, considering that ice-rafted debris reached lower latitudes at Oi-1 time than it does now[21]. The lack of ice-rafted debris in the North Atlantic (south of the Greenland–Scotland Ridge) before 2.6 Myr (ref. 37) suggests that northern-hemisphere ice sheets were not much larger than today (~7 m sea-level equivalent[38]). Assuming that there were small (~10-m-sea-level-equivalent) northern-hemisphere ice sheets, this requires growth of an Antarctic sheet that was 20% larger than it is today. This bipolar glaciation caused a ~105 m relative sea-level and ~67 m eustatic fall.

The calibration of 0.12‰/10 m requires ice sheets that were more negative (−45‰) than today for Greenland (−39‰), and similar to modern-day Antarctica (−35‰ to −60‰) (ref. 36). This is reasonable considering that (1) there are large uncertainties (~10–20‰) in previous calibrations (see above) and (2) our calibration of 0.12‰/10 m and mean ice of −45‰ is close to that expected for Antarctica today[36]. Furthermore, the isotopic composition of ice is sensitive to changes in water-vapour source. Empirical evidence suggests that meridional water-vapour $\delta^{18}O$ values were lower at Cretaceous mid-latitudes (the present-day moisture source to polar regions) owing to an enhanced hydrologic cycle and greenhouse values ~4‰ lower than modern values[39]; thus, ice may have had slightly lower $\delta^{18}O$ values. Further empirical and modelling studies are needed to evaluate ice-sheet composition in greenhouse climates.

In contrast to the 1.2‰ δ_w increase noted here, Lear and colleagues[9] estimate a 0.6‰ δ_w increase for the coeval interval (33.8–33.5 Myr), on the basis of planktonic foraminiferal $\delta^{18}O$ ($\delta^{18}O_{pf}$) and planktonic and benthic foraminiferal Mg/Ca data

from Tanzanian shelf sediments. The discrepancy between the records is minor at EOT-1 (~0.4 versus 0.2‰), yet may indicate that the ice-growth event at ~33.8 Myr is better recorded at SSQ and Sites 1218 and 522 than Tanzania. The difference at Oi-1 is more substantial: the 0.4‰ $\delta^{18}O_{pf}$ increase (sea-surface signal) and no temperature change at Tanzania[9] contrasts sharply with our 1.0‰ $\delta^{18}O_{bf}$ increase (seafloor signal) and 2 °C temperature change at SSQ, resulting in a $\sim 0.3 \pm 0.1$‰ δ_w difference between sites. We suggest that the Tanzanian 0.4‰ δ_w increase for Oi-1 must underestimate the global signal, because it cannot be reconciled with the sea-level record (see above) or our datasets. The Tanzanian section may be undersampled (one sample per metre) relative to the SSQ record (one sample per 3–20 cm) across the E–O transition, and therefore may not record the full magnitude of δ_w change. Alternatively, the Tanzanian $\delta^{18}O_{pf}$ record may be influenced by local sea-surface hydrographic changes adjacent to the continent that resulted from the ~105 m relative sea-level (~67 m eustatic) fall. In contrast, the SSQ $\delta^{18}O_{bf}$ (seafloor) record seems to be unaffected by local hydrographic changes (see above), which would be more likely to influence sea-surface conditions near continental margins. Therefore, we conclude that SSQ more accurately records global changes across the greenhouse-to-icehouse transition.

Myriad factors may have contributed to the fundamental switch in climate mode from greenhouse to icehouse, including opening of tectonic gateways that led to the thermal isolation of Antarctica[4,16], atmospheric CO_2 levels that declined below a critical threshold[40] and ice-climate feedbacks related to the orbital long-obliquity and long-eccentricity minima (cool high-latitude summers during times of low summer insolation)[8,41]. Some combination of factors may ultimately have tipped the climate balance into the icehouse world. Even in a new climate state, substantial ice-volume fluctuations continued through the Oligocene, with ice sheets that ranged from as large as today[17,42] to nearly ice-free conditions[43].

METHODS

SSQ was deposited in a mixed siliciclastic–carbonate environment on the middle to outer continental shelf. The excellent magnetobiostratigraphic age control (varying from ±0.1 to ±0.5 Myr) indicates that deposition was essentially continuous (on the 10^5–10^6 yr-scale) across the Eocene–Oligocene transition; although the section above and below the transition is punctuated by three sequence boundaries at ~50.3, 47, and 40.5 m, only the first has a detectable hiatus (Fig. 1). Integrated benthic foraminiferal biofacies and lithofacies studies show that this section was deposited in palaeodepths of ~75–125 m (ref. 18).

Sediment samples were soaked in a sodium metaphosphate solution to disaggregate the sediment, washed through a 63-μm mesh sieve and oven-dried. Benthic foraminifera were picked from the >150-μm fraction. We measured $\delta^{18}O$ and Mg/Ca in well-preserved benthic foraminifera (*Cibicidoides pippeni* and *C. cocoaensis*). Our high-resolution $\delta^{18}O_{bf}$ record (one sample per 3–60 cm) builds on a low-resolution $\delta^{18}O_{bf}$ dataset (one sample per 30–150 cm) (ref. 18). All δ_w were calculated for this study using the palaeotemperature equation of Epstein and colleagues[44] (*Cibicidoides* $\delta^{18}O$ were corrected to *Oridorsalis* $\delta^{18}O$ (ref. 45), which is assumed to faithfully record δ_w (ref. 46)): (1) Site 522 data were interpolated at 5 kyr intervals using $\delta^{18}O_{bf}$ (ref. 7) and Mg/Ca (ref. 23) because these data were not measured on the same samples; (2) Site 1218 uses $\delta^{18}O_{bf}$ (ref. 8) and Mg/Ca (ref. 17).

Benthic-foraminiferal stable-isotope analyses were conducted in the Stable Isotope Laboratory in the Department of Earth and Planetary Sciences at Rutgers University. Approximately two to ten specimens of benthic foraminifera of the genus *Cibicidoides* (*Cibicidoides pippeni*, *Cibicidoides cocoaensis* or *Cibicidoides* spp.) were selected from each sample for analysis. Foraminifera were reacted in phosphoric acid at 90 °C for 15 min in an automated peripheral attached to a Micromass Optima mass spectrometer. Stable isotope values are reported versus V-PDB by analysing NBS-19 and an internal laboratory standard during each automated run. We use the published values for NBS-19 of −2.20 and 1.95‰ for $\delta^{18}O$ and $\delta^{13}C$, respectively[47]. The one-sigma precisions of the standards analysed during automated runs are 0.08 and 0.05‰ for $\delta^{18}O$ and $\delta^{13}C$, respectively.

Foraminifera were cleaned using typical procedures for obtaining trace-metal ratios in benthic foraminifera[48]. The procedure included a clay–removal step, a manual extraction of contaminant phases using a binocular microscope, two oxidation steps, a reductive step and one dilute-acid leach. Foraminiferal Mg/Ca ratios were measured using high-resolution inductively-coupled-plasma mass spectrometry at the Institute or Marine and Coastal Sciences at Rutgers University (long-term precision < 2‰ relative standard deviation). Seafloor water temperatures were calculated from Mg/Ca ratios of benthic foraminifera using the calibration of ref. 48, and assuming seawater $Mg/Ca = 4.3\ mol\ mol^{-1}$ (ref. 49). The calibration of Marchitto and colleagues was not used because it yielded unrealistic temperatures (~45 °C), and may not be valid for shallow-water sections.

The timescale of ref. 50 is used.

Received 14 November 2007; accepted 17 March 2008; published 13 April 2008.

References

1. Pagani, M., Zachos, J. C., Freeman, K. H., Tipple, B. & Bohaty, S. Marked decline in atmospheric carbon dioxide concentrations during the Paleogene. *Science* **309**, 600–603 (2005).
2. Miller, K. G., Fairbanks, R. G. & Mountain, G. S. Tertiary oxygen isotope synthesis, sea level history, and continental margin erosion. *Paleoceanography* **2**, 1–19 (1987).
3. Zachos, J. C., Pagani, M., Sloan, L., Thomas, E. & Billups, K. Trends, rhythms, and aberrations in global climate change 65 Ma to present. *Science* **292**, 686–293 (2001).
4. Kennett, J. P. Cenozoic evolution of antarctic glaciation, the Circum-Antarctic Ocean, and their impact on global paleoceanography. *J. Geophys. Res.* **82**, 3843–3860 (1977).
5. Miller, K. G., Wright, J. D. & Fairbanks, R. G. Unlocking the Ice House: Oligocene–Miocene oxygen isotopes, eustasy, and margin erosion. *J. Geophys. Res.* **96**, 6829–6848 (1991).
6. Miller, K. G. *et al.* The phanerozoic record of global sea-level change. *Science* **310**, 1293–1298 (2005).
7. Zachos, J. C., Quinn, T. M. & Salamy, S. High resolution (10^4 yr) deep-sea foraminiferal stable isotope records of the earliest Oligocene climate transition. *Paleoceanography* **9**, 353–387 (1996).
8. Coxall, H. K., Wilson, P. A., Palike, H., Lear, C. H. & Backman, J. Rapid stepwise onset of Antarctic glaciation and deeper calcite compensation in the Pacific Ocean. *Nature* **433**, 53–57 (2005).
9. Lear, C. H., Bailey, T. R., Pearson, P. N., Coxall, H. K. & Rosenthal, Y. Cooling and ice growth across the Eocene–Oligocene transition. *Geology* **36**, 251–254 (2008).
10. Browning, J. V., Miller, K. G. & Pak, D. K. Global implications of lower to middle Eocene sequence boundaries on the New Jersey coastal plain; the icehouse cometh. *Geology* **24**, 639–642 (1996).
11. Sagnotti, L., Florindo, F., Verosub, K. L., Wilson, G. S. & Roberts, A. P. Environmental magnetic record of Antarctic palaeoclimate from Eocene/Oligocene glaciomarine sediments, Victoria Land Basin. *Geophys. J. Int.* **134**, 653–662 (1998).
12. Tripati, A., Backman, J., Elderfield, H. & Ferretti, P. Eocene bipolar glaciation associated with global carbon cycle changes. *Nature* **436**, 341–346 (2005).
13. Miller, K. G., Wright, J. D. & Browning, J. V. Visions of ice sheets in a greenhouse world. *Mar. Geol.* **217**, 215–231 (2005).
14. Prothero, D. R., Ivany, L. C. & Nesbitt, E. A. (eds) *From Greenhouse to Icehouse: The Marine Eocene–Oligocene Transition* (Columbia Univ. Press, New York, 2003).
15. Pearson, P. N. *et al.* Extinction and environmental change across the Eocene–Oligocene boundary in Tanzania. *Geology* **36**, 179–182 (2008).
16. Kennett, J. P. & Shackleton, N. J. Oxygen isotopic evidence for the development of the psychrosphere 38 Myr ago. *Nature* **260**, 513–515 (1976).
17. Lear, C. H., Rosenthal, Y., Coxall, H. K. & Wilson, P. A. Late Eocene to early Miocene ice sheet dynamics and the global carbon cycle. *Paleoceanography* **19** doi:10.1029/2004PA001039 (2004).
18. Miller, K. G. *et al.* Eocene–Oligocene global climate and sea-level changes: St. Stephens Quarry, Alabama. *GSA Bull.* **12**, 34–53 (2008).
19. Tauxe, L. P. & Hartl, P. 11 million years of Oligocene geomagnetic field behavior. *Geophys. J. Int.* **128**, 217–229 (1997).
20. Miller, K. G., Feigenson, M. D., Kent, D. V. & Olsson, R. K. Oligocene stable isotope (87Sr/86Sr, d18O, d13C) standard section, Deep Sea Drilling Project Site 522. *Paleoceanography* **3**, 223–233 (1988).
21. Zachos, J. C., Breza, J. & Wise, S. W. Jr. Early Oligocene ice-sheet expansion on Antarctica, sedimentological and isotopic evidence from Kerguelen Plateau. *Geology* **20**, 569–573 (1992).
22. Miller, K. G., Thompson, P. R. & Kent, D. V. Integrated stratigraphy of the Alabama coastal plain: Relationship of upper Eocene to Oligocene unconformities to glacioeustatic change. *Paleoceanography* **8**, 313–331 (1993).
23. Lear, C. H., Elderfield, H. & Wilson, P. A. Cenozoic deep-sea temperatures and global ice volumes from Mg/Ca in benthic foraminiferal calcite. *Science* **287**, 269–272 (2000).
24. Billups, K. & Schrag, D. P. Application of benthic foraminiferal Mg/Ca ratios to questions of Cenozoic climate change. *Earth Planet. Sci. Lett.* **209**, 181–195 (2003).
25. van Andel, T. H. & Moore, T. C. Jr. Cenozoic calcium carbonate distribution and calcite compensation depth in the central equatorial Pacific. *Geology* **2**, 87–92 (1974).
26. Dupont-Nivet, G. *et al.* Tibetan plateau aridification linked to global cooling at the Eocene–Oligocene transition. *Nature* **445**, 635–638 (2007).
27. Zanazzi, A., Kohn, M. J., MacFadden, B. J. & Terry, J., O. Large temperature drop across the Eocene–Oligocene transition in central North America. *Nature* **445**, 639–642 (2007).
28. Kominz, M. A. & Pekar, S. F. Oligocene eustasy from two-dimensional sequence stratigraphic backstripping. *Geol. Soc. Am. Bull.* **113**, 291–314 (2001).
29. Levitus, S. *NOAA Professional Paper 13* (US Government Printing Office, Washington, 1982).
30. Conkright, M. E. *et al. World Ocean Atlas: Nutrient and Chlorophyll of the Atlantic Ocean* (US Government Printing Office, Washington, 1998).
31. Kobashi, T., Grossman, E. L., Dockery, D. T. III & Ivany, L. C. Water mass stability reconstructions from greenhouse (Eocene) to icehouse (Oligocene) for the northern Gulf Coast continental shelf (USA). *Paleoceanography* **19** doi:10.1029/2003PA000934 (2004).
32. <http://www7300.nrlssc.navy.mil/altimetry/regions/reg_gom.html>, NRLSSC.
33. Brinkhuis, H. & Visscher, H. in *Geochronology, Timescales and Global Stratigraphic Correlation* (eds Berggren, W. A., Kent, D. V., Aubry, M.-P. & Hardenbol, J.) 295–304 (Society of Economic Paleontologists and Mineralogists, 1995).
34. Fairbanks, R. G. & Matthews, R. K. The marine oxygen isotopic record in Pleistocene coral, Barbados, West Indies. *Quat. Res.* **10**, 181–196 (1978).

35. Pekar, S. F., Christie-Blick, N., Kominz, M. A. & Miller, K. G. Calibration between eustatic estimates from backstripping and oxygen isotopic records for the Oligocene. *Geology* **30**, 903–906 (2002).
36. Blunier, T. & Brook, E. J. Timing of millennial-scale climate change in Antarctica and Greenland during the last glacial period. *Science* **291**, 109–112 (2001).
37. Shackleton, N. J. *et al*. Oxygen isotope calibration of the onset of ice-rafting and history of glaciation in the North Atlantic region. *Nature* **307**, 620–623 (1984).
38. Williams, R. S. Jr & Ferrigno, J. G. (eds) *Satellite Image Atlas of Glaciers of the World* (US Geological Survey Professional Paper, Vol. 1386-C, 1999).
39. White, T., González, L., Ludvigson, G. & Poulsen, C. Middle Cretaceous greenhouse hydrologic cycle of North America. *Geology* **29**, 363–366 (2001).
40. De Conto, R. & Pollard, D. Rapid Cenozoic glaciation of Antarctica induced by declining atmospheric CO_2. *Nature* **421**, 245–249 (2003).
41. Pälike, H. *et al*. The heartbeat of the Oligocene climate system. *Science* **314**, 1894–1898 (2006).
42. Wade, B. S. & Pälike, H. Oligocene climate dynamics. *Paleoceanography* **19** doi:10.1029/2004PA001042 (2004).
43. Pekar, S. F., DeConto, R. M. & Harwood, D. M. Resolving a Late Oligocene conundrum: Deep-sea warming and Antarctic glaciation. *Palaeogeogr. Palaeoclimatol. Palaeoecol.* **231**, 29–40 (2006).
44. Epstein, S., Buchsbaum, R., Lowenstam, H. A. & Urey, H. C. Revised carbonate–water isotopic temperature scale. *Geol. Soc. Am. Bull.* **64**, 1315–1326 (1953).
45. Katz, M. E. *et al*. Early Cenozoic benthic foraminiferal isotopes: Species reliability and interspecies correction factors. *Paleoceanography* **18** (2003).
46. Shackleton, N. J., Hall, M. A. & Boersma, A. Jr. in *Init. Repts. DSDP* (eds Moore, T. C. & Rabinowitz, P. D.) 599–612 (1984).
47. Coplen, T. B. Discontinuance of SMOW and PDB. *Nature* **375**, 285 (1995).
48. Lear, C., Rosenthal, Y. & Slowey, N. Benthic foraminiferal Mg/Ca-paleothermometry: A revised core-top calibration. *Geochim. Cosmochim. Acta* **66**, 3375–3387 (2002).
49. Wilkinson, B. H. & Algeo, T. J. Sedimentary carbonate record of calcium–magnesium cycling. *Am. J. Sci.* **289**, 1158–1194 (1989).
50. Berggren, W. A., Kent, D. V., Swisher, C. C. & Aubry, M.-P. in *Geochronology, Time Scales and Global Stratigraphic Correlations: A Unified Temporal Framework for an Historical Geology* (eds Berggren, W. A., Kent, D. V. & Hardenbol, J.) 129–212 (SEPM (Society for Sedimentary Geology), Tulsa, 1995).

Supplementary Information accompanies this paper on www.nature.com/naturegeoscience.

Acknowledgements

This research was supported by NSF grants OCE 06-23256 (M.E.K., K.G.M., B.S.W., J.D.W.), EAR03-07112 (K.G.M.) and EAR05-06720 (K.G.M.).

Author information

Reprints and permission information is available online at http://npg.nature.com/reprintsandpermissions.
Correspondence and requests for materials should be addressed to M.E.K.